Journal of the Korean Society of Remote Sensing, Vol. 12, No.1, 1996

대기 굴절이 고해상도 영상에 미치는 영향

신 동 석

한국과학기술원 인공위성연구센터 원격탐사 시스템 개발팀

Effects of Atmospheric Refraction on High Resolution Image Geometry

Dongseok Shin

Remote Sensing System Development Team, SaTReC, KAIST

dshin@krsc.kaist.ac.kr

Abstract

The effects of atmospheric refraction of rays on the geometry of high-resolution images such as the KOMPSAT-EOC images are described. An atmospheric refraction mechanism is modelled and the geometric errors caused by the refraction are calculated from the model simulation. This paper shows that a maximum geometric error of 1 pixel (*7m*) occurs from the standard atmospheric condition. Severer geometric distortions in images cause from an atmospheric abnormality.

요 약

이 논문에서는 대기 굴절이 다목적 실용 위성 영상과 같은 고해상도 영상의 기하학적 성질에 미치는 영향이 연구되었다. 대기 굴절 모델이 유도 되었고, 기준 대기 모델을 사용하여 영상의 기하학적 오차를 시뮬레이션을 통하여 구하였다. 표준 대기 중에서 최대 약 *7m* (1 pixel의 크기)의 오차가 대기 굴절에 의해 발생하며 이상 대기 상에서는 더 큰 오차를 일으킬 수도 있을 것이다.

1996년 5월 10일 접수 ; 1996년 6월 15일 수리.

1. Introduction

Any light, IR (infrared) or microwave signal, bends while it passes through the Earth's atmosphere due to the continuously varying refractive index of the atmosphere. This effect is taken into account when high-resolution sensors are used with considerable off-nadir viewing angles and/or stereoscopic coverage (Moccia and Vetrella, 1986).

The propagation of short waves ($< 10m$ in wavelength) is affected by neither Earth's magnetic fields nor the ionized layers of the atmosphere. As far as optical or IR waves are concerned, therefore, the refractive index is related only to the dielectric constant of the atmosphere (Castel, 1966).

Atmospheric refractivity depends on geographical location and meteorological condition. However, a standard atmosphere which represents the mean climate in temperate latitudes, was defined by CCIR (International Radio Consultative Committee) such that the exponentially varying refractive index n with height :

$$n = 1 + 289e^{-0.136h} \times 10^{-6} \quad \text{..... (1)}$$

where h is the height from the ground level in km.

KOMPSAT (Korea Multi-Purpose Satellite) is an Earth-monitoring satellite which is scheduled to be launched in 1999. Its orbit is planned to be sunsynchronous with a nominal altitude of $685km$. It carries on EOC (Electro-Optical Camera) which is an optical sensor with a high horizontal resolution of 7-10 m depending on the off-nadir viewing angle. The nominal image swath is $15km$, resulting from a maximum off-nadir viewing angle of $\pm 0.627°$. It will also provide stereoscopic images by rolling the satellite platform by as much as 45° (KARI, 1996).

The image geometry distortion caused by the atmospheric beam refraction cannot be ignored for high-precision mapping and DEM (Digital Elevation Model) generation using high-resolution satellite images such as KOMPSAT-EOC images. In this study, the geometric errors caused by the atmospheric refraction are derived and simulated for KOMPSAT-EOC images.

An atmospheric refraction model is derived in a geometric and mathematical form in Section 2. The standard atmosphere is described in Section 3. The geometric errors caused by the atmospheric refraction are simulated in Section 4. Conclusions and discussions are described in Section 5.

2. Atmospheric refraction model

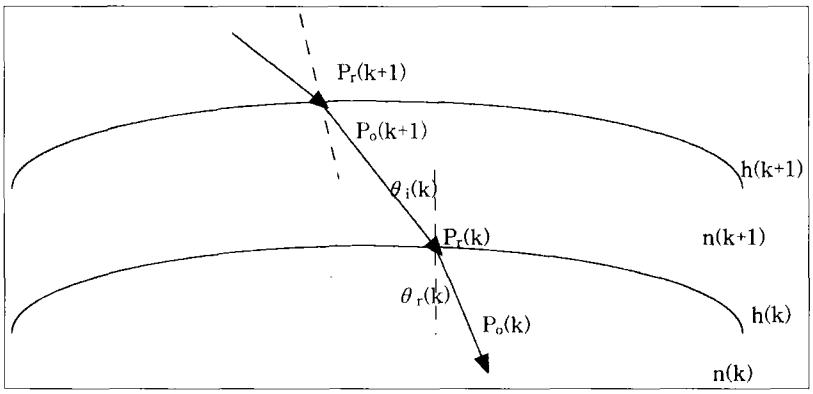

Figure 1. Atmospheric refraction model.

In Figure 1, let $P_o(k)$ be the unit vector in the direction of the ray in the k-th layer and $P_r(k)$ be the point of refraction between the $(k+1)$-th layer and k-th layer. The $P_o(k)$ can be derived in a mathematical form sequentially for every k by using the directional vector and the refractive index of each layer. The projected position of the refracted beam, $P_r(0)$, is compared with that of a straight beam for deriving the geometric error caused by the atmospheric refraction. The procedure is described in the following subsections. The vectors denoted in the subsections are based on a geocentric coordinate system with the origin at the center of the Earth.

2.1 Point of refraction $P_r(k)$

Let $P_r(k) = (x, y, z)$, $P_o(k+1) = (x_p, y_p, z_p)$, and $P_r(k+1) = (x_o, y_o, z_o)$. The point of refraction $P_r(k)$ is the crossing point of the line through $P_r(k+1)$ in the direction of $P_o(k+1)$ and the spherical atmospheric layer.

$$(x, y, z) = a(x_p, y_p, z_p) + (x_o, y_o, z_o) \quad \text{..... (2)}$$

$$x^2 + y^2 + z^2 = [R+h(k)]^2$$

where R is the radius of the Earth and $h(k)$ is the height of the top of the k-th layer. From Equation (2) :

$$a = \frac{-B - \sqrt{B^2 - AC}}{A} \quad \text{.....(3)}$$

where

$$\begin{aligned} A &= x^2_p + y^2_p + z^2_p = 1 \\ B &= x_p x_o + y_p y_o + z_p z_o \\ C &= x^2_o + y^2_o + z^2_o - [R + h(k)]^2 \end{aligned} \quad \text{.....(4)}$$

Therefore, $P_r(k)$ is obtained by the above three equations.

2.2 Incident and refracted angles

Let $P_e(k)$ be the unit vector which is normal to the top of the k-th layer at $P_r(k)$ and toward the center of the Earth.

$$P_e(k) = \frac{-P_r(k)}{|P_r(k)|} \quad \text{.....(5)}$$

The incident angle from the $(k+1)$th layer into the k-th layer is,

$$\theta_i(k+1) = \cos^{-1}(P_o(k+1) \cdot P_e(k)) \quad \text{.....(6)}$$

The refracted angle is obtained by Snell's law, which is

$$\theta_r(k) = \sin^{-1}\left(\sin(\theta_i(k+1)) \times \frac{n(k+1)}{n(k)}\right) \quad \text{.....(7)}$$

where $n(k)$ is the mean refractive index of the k-th atmospheric layer.

2.3 Refracted pointing vector

The $P_o(k)$ satisfies the following three equations:

$$\begin{aligned} P_o(k) \cdot P_o(k+1) &= \cos(\theta_i(k) - \theta_r(k)) \\ P_o(k) \cdot P_e(k) &= \cos(\theta_r(k)) \\ P_o(k) \cdot [P_o(k+1) \times P_e(k)] &= 0 \end{aligned} \quad \text{.....(8)}$$

The first and the second equations in Equation (6) were derived according to the Cosine rule as the pointing vectors are unit vectors. The last equation in Equation (6) means that the three vectors in the equation are co-planar. The above equations can be solved by three dimensional linear matrix operations.

3. Atmospheric temperature and pressure model

A theory (Lamont, 1948), based on the molecular polarization of the gases of the atmosphere, enables the refractive index to be related to the temperature T in Kelvin, pressure p in millibars, and vapour pressure e in millibars :

$$n = 1 + \frac{77.6}{T}\left(p + 4810\frac{e}{T}\right) \times 10^{-6} \quad \text{..... (9)}$$

The US standard atmosphere (COESA, 1967) is based on piecewise linear models of the variation of temperature with geopotential altitude. Pressure is computed from temperature profiles assuming the atmosphere is in the hydrostatic equilibrium, horizontally stratified, and the perfect gas law is applicable. The atmospheric temperature profile shows a large latitudal variation. Its seasonal variation is large only at high latitudes (> 60N(S)). The US stardard atmosphere was defined as the atmosphere with the seasonal average of the temperature and pressure profiles at the latitude of 45N. This atmospheric model would be appropriate for modelling the atmosphere over Korea. This is tabulated in Table 1.

4. Simulation results

The procedure described in Section 2 was repeated to calculate the point of refraction on the Earth's surface, $P_r(0)$. The initial $P_r(\infty)$ was the position of the satellite and the initial $P_o(\infty)$ was calculated from the off-nadir viewing angle ranging from 0° to 50° considering the maximum range of the roll steering angle of KOMPSAT. In the simulation, the atmosphere was divided into 32 layers taking into account the density of the atmosphere with respect to the height[1]. The refractive index of the standard atmosphere described in Section 3 was assigned to each layer. The

1) Conventionally, the top of the atmosphere is regarded as approximately 30*km*

Table 1. Temperature, pressure and refractive index of the standard atmosphere.

Altitude (km)	Temperature (K)	Pressure (mb)	$(n-1)\times10^6$
0	288.16	1013.25	277.19
1	281.66	898.76	251.55
2	275.16	795.01	227.76
3	268.67	701.21	205.74
4	262.18	616.60	185.40
5	255.69	540.48	166.63
6	249.20	472.17	149.36
7	242.71	411.05	133.51
8	236.23	356.51	118.97
9	229.74	308.00	105.68
10	223.26	265.00	93.57
11	216.78	227.00	82.55
12	216.66	193.99	70.58
13	216.66	165.79	60.32
14	216.66	141.70	51.56
15	216.66	121.12	44.07
16	216.66	103.53	37.67
17	216.66	88.50	32.20
18	216.66	75.65	27.53
19	216.66	64.67	23.53
20	216.66	55.29	20.12
21	216.66	47.27	17.20
22	216.66	40.42	14.71
23	216.66	34.56	12.58
24	216.66	29.55	10.75
25	216.66	25.27	9.20
26	219.34	21.63	7.77

division was (Shin, 1995) :

- 0 - 25*km* : 1*km* step
- 25 - 50*km* : 5*km* step
- 50 - 70*km*
- 70 - 100*km*

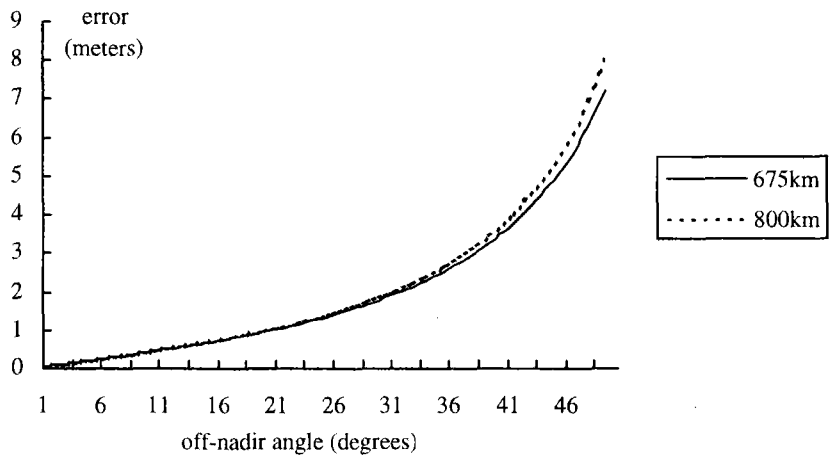

Figure 2. Geometric errors caused by the atmospheric refraction

Figure 2 shows the positional errors, i.e. positional differences between the ground projections of the refracted ray and the non-refracted ray, with respect to the off-nadir angles. The error increases with the off-nadir viewing angle and the height of the satellite. The graph shows that a pixel-level error of approximately 7 *m* occurs during the stereoscopic image acquisition of KOMPSAT-EOC using the 45° roll steering mode.

5. Conclusions and discussions

The effects of atmospheric refraction on KOMPSAT-EOC image geometry are discribed in this paper. A maximum geometric error of 1 pixel is expected from standard atmospheric conditions.

Since the main mode of KOMPSAT for the stereoscopic imaging utilizes the roll steering angle of 30° (KARI, 1996), a sub-pixel geometric error of approximately 2 *m* would be the major concern for the accurate DEM generation.

Molecules of water are easily polarized in the case of very short wavelengths, and this raises the dielectric constant of water vapour to a high value. Therefore, high-resolution images such as KOMPSAT-EOC images suffer severer geometric distortion by non-standard atmosphere containing a large amount of water vapour (e.g. tropical erea) compared with the distortion caused by the standard atmosphere.

Acknowledgement

The author would like to thank to Dr. Yongseung Kim in Korea Aerospace Research Institute for thorough reviewing of the paper and valuable advice on the atmospheric modelling.

References

Castel F.D., 1966. *Tropospheric radiowave propagation beyond the horizon*, Pergamon Press.

COESA (Committee on Extension to the Standard Atmosphere), 1967. US *Standard Atmosphere Supplements 1966*, US Government Printing Office, Washington, D.C..

KARI, 1996. *KOMPSAT PDR Report*, Korea Aerospace Research Institute.

Lamont J., 1948. Atmospheric absorption of millimeter waves, *Proc. Phys. Soc.*, 51:562-568.

Moccia A. and S. Vetrella, 1986. An integrated approach to geometric precision processing of spaceborne high-resolution sensors, *Int. J. Remote Sensing*, 7:349-359.

Shin D., 1995. *Applications of machine vision to cloud studies using stereoscopic satellite images*, PhD Thesis, University College London, 1995.